

## Arene–Mercury Complexes Stabilized by Gallium Chloride: Relative Rates of H/D and Arene Exchange

Catherine S. Branch and Andrew R. Barron\*

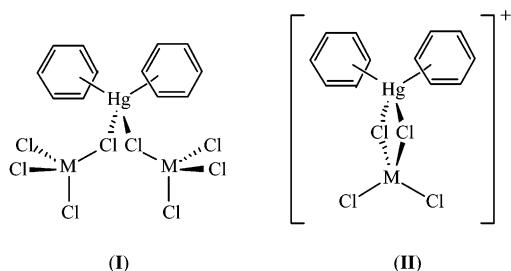
Contribution from the Department of Chemistry and Center for Nanoscale Science and Technology, Rice University, Houston, Texas 77005

Received May 6, 2002

**Abstract:** We have previously proposed that the  $\text{Hg}(\text{arene})_2(\text{GaCl}_4)_2$  catalyzed H/D exchange reaction of  $\text{C}_6\text{D}_6$  with arenes occurs via an electrophilic aromatic substitution reaction in which the coordinated arene protonates the  $\text{C}_6\text{D}_6$ . To investigate this mechanism, the kinetics of the  $\text{Hg}(\text{C}_6\text{H}_5\text{Me})_2(\text{GaCl}_4)_2$  catalyzed H/D exchange reaction of  $\text{C}_6\text{D}_6$  with naphthalene has been studied. Separate second-order rate constants were determined for the 1- and 2-positions on naphthalene; that is, the initial rate of H/D exchange =  $k_{11}[\text{Hg}][\text{C}-\text{H}_1] + k_{21}[\text{Hg}][\text{C}-\text{H}_2]$ . The ratio of  $k_{11}/k_{21}$  ranges from 11 to 2.5 over the temperature range studied, commensurate with the proposed electrophilic aromatic substitution reaction. Observation of the reactions over an extended time period shows that the rates change with time, until they again reach a new and constant second-order kinetics regime. The overall form of the rate equation is unchanged: final rate =  $k_{1f}[\text{Hg}][\text{C}-\text{H}_1] + k_{2f}[\text{Hg}][\text{C}-\text{H}_2]$ . This change in the H/D exchange is accompanied by ligand exchange between  $\text{Hg}(\text{C}_6\text{D}_6)_2(\text{GaCl}_4)_2$  and naphthalene to give  $\text{Hg}(\text{C}_{10}\text{H}_8)_2(\text{GaCl}_4)_2$ , that has been characterized by  $^{13}\text{C}$  CPMAS NMR and UV–visible spectroscopy. The activation parameters for the ligand exchange may be determined and are indicative of a dissociative reaction and are consistent with our previously calculated bond dissociation for  $\text{Hg}(\text{C}_6\text{H}_5)_2(\text{AlCl}_4)_2$ . The initial  $\text{Hg}(\text{arene})_2(\text{GaCl}_4)_2$  catalyzed reaction of naphthalene with  $\text{C}_6\text{D}_6$  involves the deuteration of naphthalene by coordinated  $\text{C}_6\text{D}_6$ ; however, as ligand exchange progresses, the pathway for H/D exchange changes to where the protonation of  $\text{C}_6\text{D}_6$  by coordinated naphthalene dominates. The site selectivity for the H/D exchange is initially due to the electrophilic aromatic substitution of naphthalene. As ligand exchange occurs, this selectivity is controlled by the activation of the naphthalene C–H bonds by mercury.

### Introduction

We have recently reported that the reaction of  $\text{HgCl}_2$  with 2 equiv. of  $\text{MCl}_3$  ( $\text{M} = \text{Al}, \text{Ga}$ ) in an aromatic solvent yields  $\text{Hg}(\text{arene})_2(\text{MCl}_4)_2$ , where arene =  $\text{C}_6\text{H}_5\text{Me}$ ,  $\text{C}_6\text{H}_5\text{Et}$ ,  $o\text{-C}_6\text{H}_4\text{Me}_2$ , and  $\text{C}_6\text{H}_3\text{-1,2,3-Me}_3$ .<sup>1,2</sup> In the solid state, these compounds exist as either neutral complexes in which two arenes are bound to the mercury and the  $\text{MCl}_3$  groups are bound through bridging chlorides to the mercury (**I**) or as a cation–anion pair (**II**). In solution, however, all the complexes exist in their neutral forms.<sup>2</sup>



Dissolution of  $\text{Hg}(\text{arene})_2(\text{MCl}_4)_2$  in  $\text{C}_6\text{D}_6$  results in a rapid H/D exchange and the formation of the appropriate  $d_n$ -arene

and  $\text{C}_6\text{D}_5\text{H}$ .<sup>3</sup> The H/D exchange reaction was found to be catalytic with respect to  $\text{Hg}(\text{arene})_2(\text{MCl}_4)_2$  and independent of the initial arene ligand. The rate of these exchange reactions is unexpectedly fast, given that they are carried out in an aprotic solvent and without a Brønsted acid.<sup>4</sup>

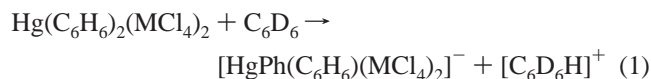
The majority of H/D exchange reactions are carried out under acid catalyzed conditions. The addition of water or a mineral acid can significantly enhance the rate of exchange between  $\text{C}_6\text{D}_6$  and  $\text{HO}_2\text{CCF}_3$ ,<sup>5</sup> whereas the addition of an aprotic Lewis acid reduces the rate of exchange.<sup>6</sup> H/D exchange reactions for aromatic compounds are also known to occur in the presence of transition metal catalysts. For example, H/D exchange between heavy water and aromatic hydrocarbons is homogeneously catalyzed by  $[\text{PtCl}_4]^{2-}$  salts.<sup>7</sup> Calderazzo et al.<sup>8</sup> have

- (1) Borovik, A. S.; Bott, S. G.; Barron, A. R. *Angew. Chem., Int. Ed.* **2000**, *39*, 4117.
- (2) Borovik, A. S.; Bott, S. G.; Barron, A. R. *J. Am. Chem. Soc.* **2001**, *123*, 11219.
- (3) Borovik, A. S.; Barron, A. R. *J. Am. Chem. Soc.* **2002**, *124*, 3743.
- (4) Although  $\text{AlCl}_3$  will catalyze the H/D exchange between  $\text{C}_6\text{D}_6$  and toluene, traces of dissolved water are involved in the proton transfer; see (a) Garrett, J. L.; Long, M. A.; Vining, R. F. *J. Chem. Soc., Chem. Commun.* **1972**, 1172. (b) Gaines, D. F.; Beall, H. *Inorg. Chem.* **2000**, *39*, 1812.
- (5) Mackor, E. L.; Smit, P. J.; van der Waals, J. H. *Trans. Faraday Soc.* **1957**, *53*, 1309.
- (6) Taylor, R. *Comprehensive Chemical Kinetics*; Elsevier: Amsterdam, 1972; Vol 13, pp 194–277.
- (7) Hodges, R. J.; Garnett, J. L. *J. Catal.* **1969**, *13*, 83.

\* To whom correspondence should be addressed: www.rice.edu/barron.

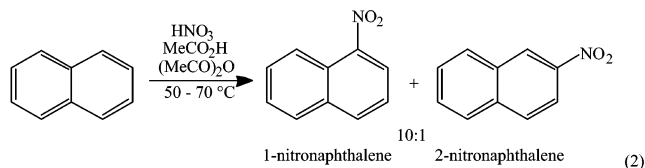
reported H/D exchange of the ring protons between  $C_6D_6$  and  $C_6H_{6-n}Me_n$  promoted by titanium(IV)–arene complexes. Gaseous deuterium can be exchanged with  $C_6H_6$  if tantalum ( $Cp_2TaH_3$ ) or iridium [ $(PhEt_2P)_2IrH_3$ ] hydrides are used as catalysts.<sup>9</sup>

On the basis of DFT calculations,<sup>3</sup> we have proposed that the reaction pathway for arene H/D exchange involves the protonation of benzene by  $Hg(C_6H_6)_2(MCl_4)_2$  and the formation of a Wheland intermediate, eq 1. Furthermore, we proposed that the coordination of the arene to the mercury/group 13 complex results in a significant increase in the acidity of the aromatic hydrogens,<sup>10</sup> sufficient to cause the coordinated arene to act as the acid in a typical electrophilic aromatic substitution reaction.



To confirm that the mechanism of H/D exchange catalyzed by  $Hg(arene)_2(MCl_4)_2$  involves an electrophilic aromatic substitution reaction, we have investigated the kinetics of the H/D exchange reaction. In particular, we are interested in comparing the site preference of the reaction with that of a well-characterized electrophilic aromatic substitution reaction.<sup>11</sup>

Naphthalene undergoes a number of usual electrophilic aromatic substitution reactions such as nitration, halogenation, sulfonation, and Friedel–Crafts acylation. Although the exact ratio of products is dependent on the reactants and the reaction conditions, the 1-position is the more reactive (e.g., eq 2).<sup>12,13</sup>



If arene H/D exchange catalyzed by  $Hg(C_6H_6)_2(MCl_4)_2$  involves an electrophilic aromatic substitution reaction, a similar site preference should be observed for the H/D exchange between  $C_6D_6$  and naphthalene. The results of this study are presented herein.

## Results and Discussion

The reaction of naphthalene ( $C_{10}H_8$ ) with excess  $C_6D_6$  in the presence of a catalytic quantity of  $Hg(C_6H_5Me)_2(GaCl_4)_2$  results in the formation of  $C_{10}D_8$  and  $C_6D_5H$ . The presence of octadeuterionaphthalene ( $C_{10}D_8$ ) is confirmed by  $^{13}C$  NMR spectroscopy and MS (see Experimental Section).

We have studied the kinetics of the  $Hg(C_6H_5Me)_2(GaCl_4)_2$  catalyzed reaction of  $C_6D_6$  with naphthalene. Even though the catalytic exchange involves  $C_6D_6$  and  $C_{10}D_8$ , we employed  $Hg(C_6H_5Me)_2(GaCl_4)_2$  as a source of  $Hg(C_6H_6)_2(GaCl_4)_2$ , rather

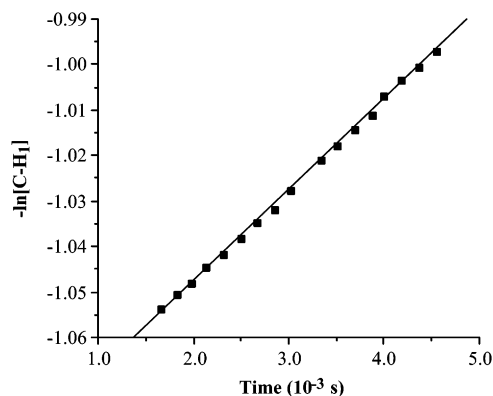
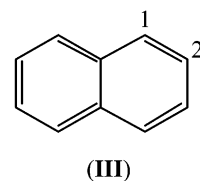


**Figure 1.** Representative plot determining the first-order rate constant for the initial H/D exchange between  $C_6D_6$  and the 1-position on  $C_{10}H_8$  ( $R = 0.991$ ).

than  $Hg(C_6H_6)_2(GaCl_4)_2$  directly. This is because the toluene complex may be isolated as a solid while the benzene complex forms a liquid clathrate.<sup>2</sup> We have previously shown that the identity of the initial arene complex is unimportant with regard to the product distribution with respect to the H/D exchange.<sup>2</sup> We proposed that this was due to the facile ligand exchange between toluene and benzene, resulting in the formation of  $Hg(C_6H_6)_2(GaCl_4)_2$  in situ. This assumption is confirmed by the present study.

In a typical experiment, 0.78 mmol of naphthalene is dissolved in 1 mL of  $C_6D_6$ , to which is added  $\sim 3 \mu\text{mol}$  of  $Hg(C_6H_5Me)_2(GaCl_4)_2$ . These quantities enable  $^1H$  NMR measurements to be made over  $\sim 3$ –12 h for runs between 20 and 65 °C and allow us to overcome the errors that occur when initial rates are measured at temperatures different from ambient. We note that only H/D exchange reactions may be followed by  $^1H$  NMR spectroscopy; degenerate H/H and D/D exchanges are not observed. Retrogressive H/D exchanges (i.e., between two naphthalene molecules) should not be significant during the early stages of the reaction and in the presence of a large excess of  $C_6D_6$ . The rate of loss of naphthalene C–H groups (and, thus, concurrent formation of naphthalene C–D groups) may be followed by  $^1H$  NMR.

Separate first-order observed rate constants,  $k_{\text{obs}}$  (eq 3), were calculated from the corresponding plot of  $-\ln[C-H_n]$  versus time (e.g., Figure 1) for the 1- and 2-positions on naphthalene, where  $[C-H_n]$  is the concentration of the hydrogen atoms at the  $n$ -position on naphthalene (**III**). A plot of  $k_{\text{obs}}$  versus the



concentration of the catalyst,  $[Hg(arene)_2(GaCl_4)_2]$ , shows a linear dependence (Figure 2), indicating the rate of H/D exchange is first order with respect to both the substrate and catalyst. An overall rate equation may be described for the initial phase of the H/D exchanges, eq 4.<sup>14,15</sup> Measurement of the temperature dependence (20–65 °C) for  $k_{1i}$  and  $k_{2i}$  (e.g., Figure

(14) We have defined  $k_{1i}$  and  $k_{2i}$  as the rate constants for the initial H/D exchange reaction.

(8) Calderazzo, F.; Pampaloni, G.; Vallieri, A. *Inorg. Chim. Acta* **1995**, 229, 179.

(9) Barefield, E. K.; Parshall, G. W.; Tebbe, F. N. *J. Am. Chem. Soc.* **1970**, 92, 5234.

(10) We have previously shown that group 13 Lewis acids, such as  $AlR_3$ , can increase the proton acidity of coordinated alcohols, as measured by a decrease in the  $pK_a$ , by at least 7 units. McMahon, C. N.; Bott, S. G.; Barron, A. R. *J. Chem. Soc., Dalton Trans.* **1997**, 3129.

(11) Taylor, R. *Electrophilic Aromatic Substitution*; Wiley: New York, 1990; Chapter 3.

(12) Makor, E. L.; Hofstra, A.; van der Waals, J. H. *Trans. Faraday Soc.* **1958**, 54, 66.

(13) Fischer, P.; Taylor, R. *J. Chem. Soc., Perkin Trans.* **1980**, 781.

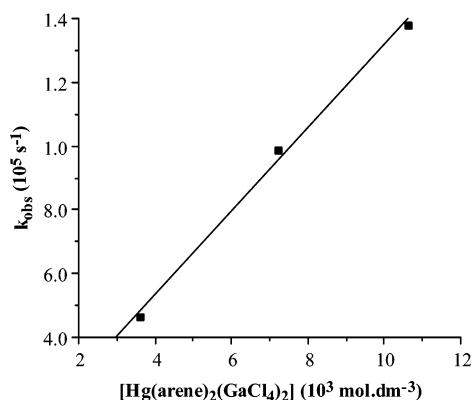


**Figure 2.** Plot of  $k_{\text{obs}}$  as a function of catalyst concentration for the initial H/D exchange between  $\text{C}_6\text{D}_6$  and the 1-position on  $\text{C}_{10}\text{H}_8$  ( $R = 0.992$ ).

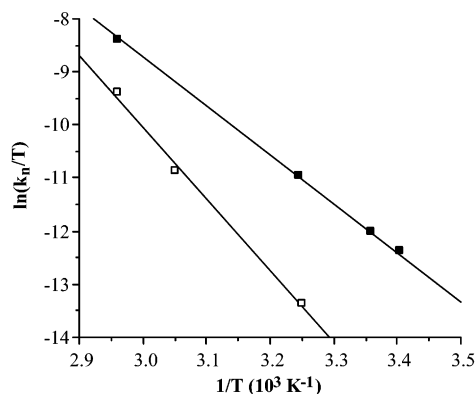


**Figure 3.** Representative Eyring plot for the initial H/D exchange between  $\text{C}_6\text{D}_6$  and the 1-position (■,  $R = 0.993$ ) and 2-position (□,  $R = 0.993$ ) on  $\text{C}_{10}\text{H}_8$ .

**Table 1.** Summary of Activation Enthalpy and Entropy for the  $\text{Hg}(\text{C}_6\text{H}_5\text{Me})_2(\text{GaCl}_4)_2$  Catalyzed H/D Exchange Reaction<sup>a</sup>

	naphthalene substituent	$k_r^b$ at 338 K ( $10^2 \text{ mol}^{-1} \text{ dm}^3 \text{ s}^{-1}$ )	$\Delta H^\ddagger$ ( $\text{kJ mol}^{-1}$ )	$\Delta S^\ddagger$ ( $\text{J K}^{-1} \text{ mol}^{-1}$ )
initial reaction	1	7.5(3)	77(1)	158(5)
	2	2.9(1)	110(10)	250(20)
final reaction	1	9.5(4)	61(2)	114(6)
	2	8.7(3)	63(5)	120(10)

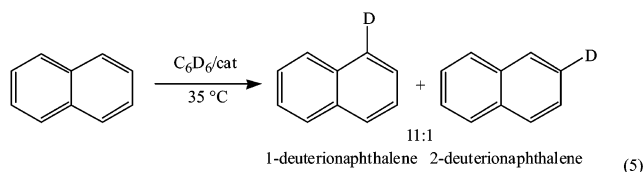
<sup>a</sup> Esd's given in parentheses. <sup>b</sup> Value calculated from thermodynamic data.

3) allows for the determination of  $\Delta H^\ddagger$  and  $\Delta S^\ddagger$  (see Table 1). The large positive value of  $\Delta S^\ddagger$  indicates a dissociative reaction.<sup>16</sup>

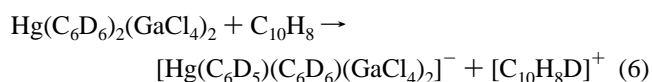
$$-d[\text{C}-\text{H}_n]/dt = k_{\text{obs}}[\text{C}-\text{H}_n] \quad (3)$$

$$\text{rate H/D exchange} = k_{1i}[\text{Hg}][\text{C}-\text{H}_1] + k_{2i}[\text{Hg}][\text{C}-\text{H}_2] \quad (4)$$

The initial H/D exchange with the 2-position is sufficiently slow at 25 °C under the conditions studied that it is not possible to measure the rate; however, above 35 °C, the relative rates may be determined and show a preferential reaction with the 1-position (e.g., eq 5).



The ratio of  $k_{1i}/k_{2i}$  ranges from 11 to 2.5 over the temperature range studied (35–65 °C). This agrees with previous proton affinity studies<sup>12,13</sup> and suggests that protonation of the naphthalene is occurring during the H/D exchange. The site selectivity for the  $\text{Hg}(\text{arene})_2(\text{GaCl}_4)_2$  catalyzed H/D exchange reaction is commensurate with an electrophilic aromatic substitution reaction. In addition, the rate equation is consistent with the protonation of naphthalene by the coordinated benzene in  $\text{Hg}(\text{C}_6\text{D}_6)_2(\text{GaCl}_4)_2$  (eq 6).



Although the rates for H/D exchange follow first-order kinetics during the first hour, observation of the reactions over an extended time period shows that the rates change with time. After an initial period, the reaction rates increase until they once again reach a new first-order kinetics regime. The final rates do not change throughout the rest of the observed reaction (e.g., Figure 4). The overall form of the rate equation is unchanged (eq 7), although the rate constants  $k_{1f}$  and  $k_{2f}$  are both increased. As may be seen from Table 1, the value for  $k_{2f}$  is closer to that of  $k_{1f}$  than during the initial reaction period (i.e.,  $k_{1i} > k_{2i}$ , while  $k_{1f} \approx k_{2f}$ ). The  $\Delta H^\ddagger$  and  $\Delta S^\ddagger$  for these reactions may be determined from the temperature dependence for  $k_{1f}$  and  $k_{2f}$  (see Table 1). As with the initial reactions, the positive values of  $\Delta S^\ddagger$  are indicative of a dissociative reaction.<sup>16</sup>

$$\text{final rate of H/D exchange} = k_{1f}[\text{Hg}][\text{C}-\text{H}_1] + k_{2f}[\text{Hg}][\text{C}-\text{H}_2] \quad (7)$$

The  $\Delta H^\ddagger$  for the H/D exchange at the 1-position is only slightly decreased between the two reaction regimes. In contrast, the  $\Delta H^\ddagger$  for the H/D exchange at the 2-position decreases significantly such that it becomes comparable to that for exchange at the 1-position. This is in direct contrast to the trend expected for an electrophilic aromatic substitution reaction on naphthalene. It would, therefore, appear that the reaction pathway changes with time. Two questions are raised from these observations. *What is the change in reaction pathway, and why does the site selectivity of the H/D exchange change?*

We have observed that, during the NMR experiments, a small quantity of a dark orange solid precipitate is observed once the H/D exchange has concluded. MS of this material shows that naphthalene is the only arene there, while <sup>13</sup>C CPMAS NMR spectroscopy and analysis indicates the composition to be  $\text{Hg}(\text{C}_{10}\text{H}_8)_2(\text{GaCl}_4)_2$  (see Figure 5). <sup>13</sup>C CPMAS NMR spectroscopic peak assignments were obtained by a combination of dipolar dephasing experiments<sup>17</sup> and comparison with calculated (DFT) chemical shifts (see Experimental Section). Figure 6 shows the calculated structure for  $\text{Hg}(\text{C}_{10}\text{H}_8)_2(\text{GaCl}_4)_2$ . Table

(15) It should be noted that the major source of error in the calculation of the individual second-order rate constants involves the measurement of the mass of catalyst.

(16) Atwood, J. D. *Inorganic and Organometallic Reaction Mechanisms*; VCH: New York, 1997; p 14.

(17) Alemany, L. B.; Grant, D. M.; Alger, T. D.; Pugmire, R. J. *J. Am. Chem. Soc.* **1983**, *105*, 6697.

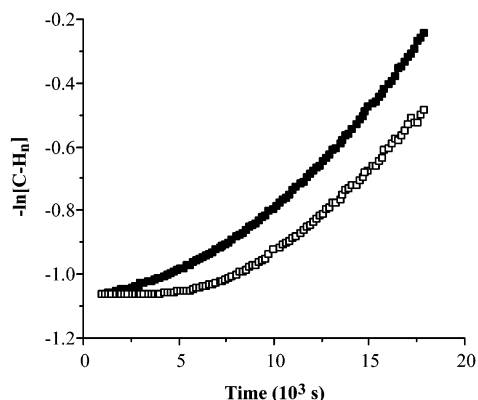


**Figure 4.** Representative plot of  $-\ln[\text{C}-\text{H}_1]$  (■) and  $-\ln[\text{C}-\text{H}_2]$  (□) versus time (s) for the  $\text{Hg}(\text{arene})_2(\text{GaCl}_4)_2$  catalyzed H/D exchange between  $\text{C}_6\text{D}_6$  and  $\text{C}_{10}\text{H}_8$  at 308 K.

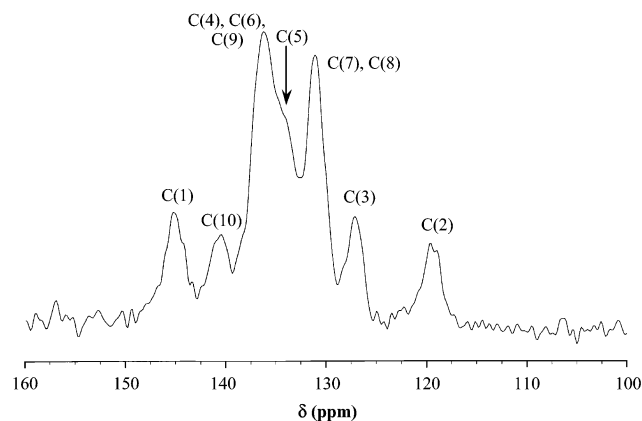


**Figure 5.**  $^{13}\text{C}$  CPMAS NMR spectra of  $\text{Hg}(\text{C}_{10}\text{H}_8)_2(\text{GaCl}_4)_2$ .

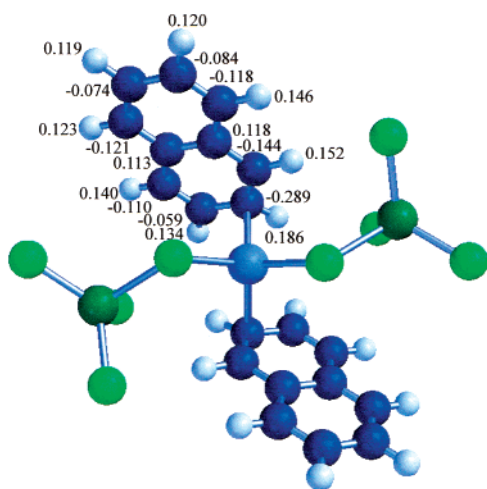


**Figure 6.** Calculated structure for  $\text{Hg}(\text{C}_{10}\text{H}_8)_2(\text{GaCl}_4)_2$  showing atom numbering scheme.

2 gives a comparison of the calculated and experimental  $^{13}\text{C}$  NMR shifts for  $\text{Hg}(\text{C}_{10}\text{H}_8)_2(\text{GaCl}_4)_2$ .

We have previously noted that, even without X-ray crystallographic data, the  $^{13}\text{C}$  CPMAS NMR spectrum of  $\text{Hg}(\text{arene})_2(\text{MCl}_4)_2$  ( $\text{M} = \text{Al}, \text{Ga}$ ) is able to provide limited structural information. First, the number of aromatic resonances observed in the  $^{13}\text{C}$  CPMAS NMR spectrum correlates well with the crystallographic symmetry. Thus, on the basis of the observation of a single set of resonances in the  $^{13}\text{C}$  CPMAS NMR spectrum

**Table 2.** Experimental and Calculated (DFT)  $^{13}\text{C}$  NMR Spectra for  $\text{Hg}(\text{C}_{10}\text{H}_8)_2(\text{GaCl}_4)_2$

atom <sup>a</sup> $\delta$ (ppm)	calculated shift $\delta$ (ppm)	experimental shift
C(1)	138.6	145
C(2)	108.0	119
C(3)	126.1	127
C(4)	134.6	136
C(5)	127.0	134
C(6)	131.7	136
C(7)	128.0	130
C(8)	128.4	130
C(9)	131.3	136
C(10)	136.2	140

<sup>a</sup> See Figure 6 for atom numbering scheme.

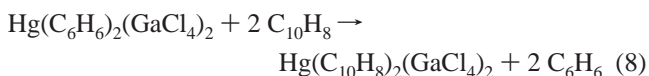
**Table 3.** Calculated Bond Lengths (Å) and Angles (°) in  $\text{Hg}(\text{arene})_2(\text{GaCl}_4)_2$

	Calcd		Exp <sup>a</sup>
	$\text{C}_{10}\text{H}_8$	$\text{C}_6\text{H}_6$	$\text{C}_6\text{H}_5\text{R}$ (R = Me, Et)
Hg–C	2.410	2.411	2.33(1)–2.249(9)
Hg···C	2.690	2.830	2.71(1)–2.75(1)
Hg–Cl	2.470	2.450	2.634(4)–2.652(2)
Ga–Cl <sub>br</sub>	2.429	2.448	2.239(2)–2.230(4)
Ga–Cl <sub>ter</sub>	2.220–2.260	2.225–2.272	2.128(4)–2.166(3)
Cl–Hg–Cl	103.63	102.86	84.5(6)–85.6(2)
C–Hg–C	101.89	108.54	126(1)–131.3(6)
Hg–Cl–Ga	116.63	119.33	110.6(1)–111.4(2)

<sup>a</sup> Borovik, A.; Bott, S. G.; Barron, A. R. *J. Am. Chem. Soc.* **2001**, *123*, 11219.

(including the dipolar dephasing experiment), we propose that  $\text{Hg}(\text{C}_{10}\text{H}_8)_2(\text{GaCl}_4)_2$  crystallizes with  $\text{C}_2$  symmetry. Second, there is a strong correlation between  $\text{Hg}\cdots\text{C}$  distance and the  $^{13}\text{C}$  chemical shift.<sup>2</sup> Thus, on the basis of the observed  $^{13}\text{C}$  chemical shifts for C(1) and C(2) (see Table 2) and using the previously reported relationship,<sup>2</sup> the  $\text{Hg}-\text{C}(2)$  and  $\text{Hg}\cdots\text{C}(1)$  distances are predicted to be 2.38 and 2.86 Å, respectively. Table 3 gives the calculated (DFT) bond lengths and angles for  $\text{Hg}(\text{C}_{10}\text{H}_8)_2(\text{GaCl}_4)_2$  and  $\text{Hg}(\text{C}_6\text{H}_5\text{R})_2(\text{GaCl}_4)_2$  along with X-ray crystallographic data for  $\text{Hg}(\text{C}_6\text{H}_5\text{R})_2(\text{GaCl}_4)_2$  (R = Me, Et). As may be seen from Table 3, the calculated  $\text{Hg}-\text{C}(2)$  and  $\text{Hg}\cdots\text{C}(1)$  distances are slightly shorter (~2%) than those predicted from  $^{13}\text{C}$  NMR spectroscopy; however, we have previously observed a similar underestimation of the  $\text{Hg}-\text{C}$  distance by DFT calculations.<sup>2</sup>

The UV–visible spectrum for  $\text{Hg}(\text{C}_{10}\text{H}_8)_2(\text{GaCl}_4)_2$  ( $\lambda = 313$  nm) is distinct from that of the toluene ( $\lambda = 305$  nm) or benzene ( $\lambda = 279$  nm) complexes. The UV–visible spectrum for a solution of  $\text{Hg}(\text{C}_6\text{H}_5\text{Me})_2(\text{GaCl}_4)_2$  in benzene shows a change with the addition of naphthalene consistent with the formation of  $\text{Hg}(\text{C}_{10}\text{H}_8)_2(\text{GaCl}_4)_2$  (i.e., eq 8).



The time at which  $\text{Hg}(\text{C}_{10}\text{H}_8)_2(\text{GaCl}_4)_2$  is dominant coincides with the point at which the H/D exchange kinetics alter from the initial to final rates. We propose, therefore, that the change in the reaction rates observed by  $^1\text{H}$  NMR accompanies ligand exchange. Since the naphthalene complex is the dominant species during the later H/D exchange reaction, we propose that the rate equation is consistent with the protonation of  $d_6$ -benzene by the coordinated naphthalene in  $\text{Hg}(\text{C}_{10}\text{H}_8)_2(\text{GaCl}_4)_2$  (eq 9).

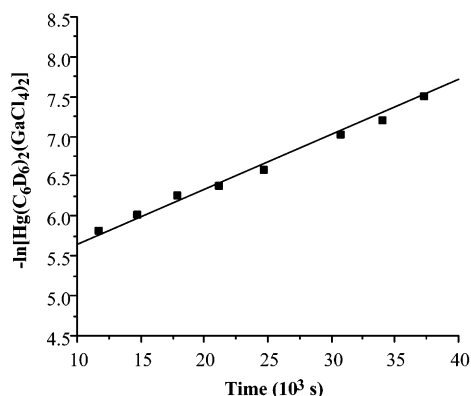
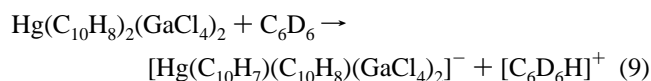
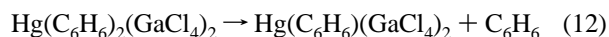
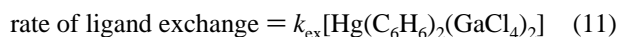
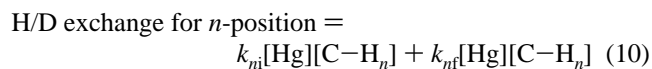


**Figure 7.** Representative plot of  $-\ln[\text{Hg}(\text{C}_6\text{D}_6)_2(\text{GaCl}_4)_2]$  versus time (s) at 298 K ( $R = 0.966$ ) for the ligand exchange between  $\text{Hg}(\text{C}_6\text{D}_6)_2(\text{GaCl}_4)_2$  and  $\text{C}_{10}\text{H}_8$ .

This is supported by the study of the H/D exchange between isolated  $\text{Hg}(\text{C}_{10}\text{H}_8)_2(\text{GaCl}_4)_2$  and  $\text{C}_6\text{D}_6$ .



We have assumed that the initial phase of the reaction is dominated by eq 6 and the final reaction is dominated by eq 9 and that the rate for H/D exchange at the  $n$ -position of the naphthalene is defined as a combined rate equation (eq 10). When the above is given and the  $^1\text{H}$  NMR data over the whole reaction is used, the concentration of  $\text{Hg}(\text{C}_6\text{H}_6)_2(\text{GaCl}_4)_2$  at time  $t$  may be determined. The rate of ligand exchange (eq 8) is determined to be first order with respect to the concentration of  $\text{Hg}(\text{C}_6\text{H}_6)_2(\text{GaCl}_4)_2$  (eq 11). First-order rate constants,  $k_{\text{ex}}$ , were calculated from the corresponding plot of  $-\ln[\text{Hg}(\text{C}_6\text{H}_6)_2(\text{GaCl}_4)_2]$  versus time. Measurement of the temperature dependence for  $k_{\text{ex}}$  (Figure 7) allows for the determination of  $\Delta H^\ddagger$  and  $\Delta S^\ddagger$  to be 63(1) kJ mol $^{-1}$  and 86(7) J K $^{-1}$  mol $^{-1}$ , respectively. The positive values of  $\Delta S^\ddagger$  are indicative of a dissociative reaction (eq 12),<sup>16</sup> while the value for  $\Delta H^\ddagger$  [63(1) kJ mol $^{-1}$ ] is consistent with our calculated bond dissociation energy ( $\Delta H = 60$  kJ mol $^{-1}$ ) for  $\text{Hg}(\text{C}_6\text{H}_6)_2(\text{AlCl}_4)_2$ .<sup>3</sup>



On the basis of the foregoing, the initial  $\text{Hg}(\text{arene})_2(\text{GaCl}_4)_2$  catalyzed reaction of naphthalene with  $d_6$ -benzene involves the deuteration of naphthalene by coordinated  $\text{C}_6\text{D}_6$  (cf., eq 6). As ligand exchange progresses, the pathway for H/D exchange changes to where the protonation of  $\text{C}_6\text{D}_6$  by coordinated naphthalene dominates (eq 9). We propose it is this change in the reaction pathway that is responsible for the apparent loss in site selectivity for the H/D exchange.

On the basis of the  $^{13}\text{C}$  CPMAS NMR spectrum for  $\text{Hg}(\text{C}_{10}\text{H}_8)_2(\text{GaCl}_4)_2$  and the calculated structure (Figure 8), it appears that there is a preference for coordination of the mercury to the 2-position of the naphthalene. Such a preferential coordination to the 2-position is predicted on steric and electronic grounds. We have previously also observed by X-ray

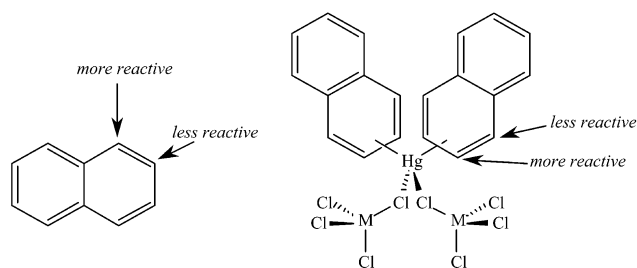


**Figure 8.** Schematic representation of the relative reactivities of the hydrogens in the 1- and 2-positions of naphthalene toward H/D exchange.

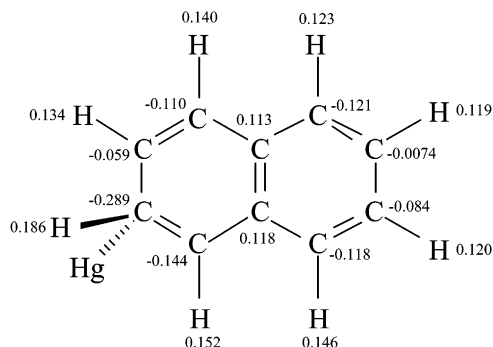


**Figure 9.** Calculated charge distribution on the aromatic C and H atoms in  $\text{Hg}(\text{C}_{10}\text{H}_8)_2(\text{GaCl}_4)_2$ .

crystallographic analysis of  $\text{Hg}(\text{C}_6\text{H}_6-n\text{Me})_2(\text{MCl}_4)_2$  that there is a similar preference for the coordination of the mercury to the carbon *para* to the arene's substituents.<sup>2</sup> On the basis of  $^{13}\text{C}$  CPMAS NMR chemical shifts<sup>2</sup> and DFT calculations,<sup>3</sup> the charge on the proton and carbon associated with the shortest  $\text{Hg}\cdots\text{C}$  interaction is significantly higher than that on free arene. The effect is also present, albeit reduced, on the C and H atoms *ortho* to the short  $\text{Hg}\cdots\text{C}$  interaction. Thus, the C–H bond on the carbon associated with mercury is the most highly activated (Figure 8). This is confirmed by observation of the calculated charge distribution on the aromatic C and H atoms for  $\text{Hg}(\text{C}_{10}\text{H}_8)_2(\text{GaCl}_4)_2$  (Figure 9).

The relative rate for the H/D exchange between naphthalene and  $\text{Hg}(\text{C}_6\text{D}_6)_2(\text{GaCl}_4)_2$  (eq 9) is controlled in the same way as that for any related electrophilic aromatic substitution reaction of naphthalene. In contrast, the relative rate for the H/D exchange between benzene and  $\text{Hg}(\text{C}_{10}\text{H}_8)_2(\text{GaCl}_4)_2$  (eq 6) is controlled by the relative activation of the naphthalene C–H bonds. Since the mercury will preferentially bind to the carbon at the 2-position, this C–H bond will be activated significantly more than the C–H bond associated with the 1-position (see Figures 8 and 9). The change in site selectivity upon ligand exchange is unfortunate in that it precludes the easy site specific H/D exchange for many arenes; however, the presence of a ligand exchange in favor of the most substituted arene does allow for the isolation of complexes previously unobtainable by direct synthesis.

The presence of ligand exchange to the more stable substituted arene also helps explain why the use of  $\text{Hg}(\text{C}_6\text{H}_5\text{Me})_2(\text{GaCl}_4)_2$  as a Friedel–Crafts catalyst (e.g., alkylation of toluene by ethylene) does not allow for complete conversion of all the toluene.<sup>18</sup> Presumably, preferential coordination of the poly-

(18) Borovik, A.; Branch, C. S.; Barron, A. R., submitted for publication.

alkylated toluene occurs such that ligand exchange with toluene to provide fresh substrate cannot occur.

## Experimental Section

Solution NMR spectra were obtained on Bruker Avance 200 and 500 spectrometers. Chemical shifts are reported relative to internal solvent resonances. NMR tubes were cleaned in basic solution, followed by an acetone wash. The tubes were dried and stored in an oven prior to use, from which they are taken directly to the port on the drybox which is immediately evacuated. The  $C_6D_6$  was predried and stored in the drybox over molecular sieves.  $^{13}C$  MAS spectra were obtained on the Bruker Avance 200 spectrometer. A 7-mm zirconium dioxide rotor was used for all spectra, with the spin rates up to 7 kHz. UV–visible spectral data were recorded on a Varian Cary 4 spectrometer. GC/MS analyses were carried out using a Finnigan MAT 95 mass spectrometer operating with an electron beam energy of 70 eV for EI mass spectra and equipped with a Hewlett-Packard 5890 series II gas chromatograph using a DB-5 30 m  $\times$  0.25 mm id column with a 0.25-mm coating of DB-5 stationary phase and injector and transfer line temperatures of 180 and 250  $^{\circ}C$ , respectively. The column was started at 35  $^{\circ}C$  for 2 min, then heated at 25  $^{\circ}C$   $min^{-1}$  for 6 min, and maintained at 185  $^{\circ}C$  for 1 min. Isotope patterns for all deuterium containing species were matched with calculated distributions. The synthesis of  $Hg(C_6H_5Me)_2(GaCl_4)_2$  was as reported previously.<sup>1,2</sup> Solvents and all arenes were distilled and degassed prior to use.

**Reaction of  $Hg(C_6H_5Me)_2(MCl_4)_2$  with  $C_{10}H_8$  in  $C_6D_6$ .** To a yellow solution of  $Hg(C_6H_5Me)_2(GaCl_4)_2$  (0.128 g, 0.158 mmol) in  $C_6D_6$  (35 g, 416 mmol) was added naphthalene (2.50 g, 19.5 mmol). The resulting orange solution was allowed to stir for 12 h. After the reaction was complete, water (5 mL) was added to deactivate the catalyst. The aromatic and aqueous layers were allowed to separate, and the aromatic layer was isolated by decanting. The solid was isolated by removing the volatiles in the aromatic layer, and its identity was confirmed by MS and  $^{13}C$  NMR.

**$C_{10}D_8$ .** MS (EI, %):  $m/z$  136 ( $M^+$ , 100), 134 ( $M^+ - H$ , 24), 132 ( $M^+ - 2H$ , 5).  $^{13}C$  NMR ( $C_6D_6$ ):  $\delta$  134.2 (s, 9-C), 128.2 [t,  $J(C-D) = 24$  Hz, 1-CD], 125.8 [t,  $J(C-D) = 24$  Hz, 2-CD].

**Catalytic H/D Exchange.** In a typical experiment, naphthalene (0.100 g, 0.78 mmol) was dissolved in  $C_6D_6$  ( $\sim 1$  mL) in a 5-mm NMR tube. To this was added  $Hg(C_6H_5Me)_2(GaCl_4)_2$  (3.00 mg, 3.71  $\mu$ mol), turning the clear solution light yellow. The sample was protected from light by a sleeve of aluminum foil because  $Hg(C_6H_5Me)_2(GaCl_4)_2$  is light sensitive. At temperatures other than 294 K, the NMR was equilibrated before the sample was inserted. Each NMR measurement yielded a spectrum consisting of two sets of naphthalene peaks and a peak due to  $C_6D_5H$ . The peaks were integrated over consistent ranges. From these integrations, the concentrations of C–H at both the 1- and 2-positions, as well as the growing  $C_6D_5H$  concentration, were determined.

The methods by which  $k_{obs}$  and  $k_n$  were determined are standard.<sup>16</sup> Because the rate of ligand exchange is sufficiently slow, under the conditions studied, the initial reaction is essentially that as described in eq 6. Thus,  $k_{obs}$  may be determined in the ordinary manner (see Figure 1). A plot of  $k_{obs}$  versus [catalyst] allows for the determination of the second-order rate constants,  $k_{11}$  and  $k_{12}$  (see Figure 2). Once ligand exchange has completed (although presumably an equilibrium, eq 8 is sufficiently shifted to the right to be an irreversible reaction), the rate constants are obtained by a similar process.

With regard to the rate of exchange of the arene ligands, we provided an explanation in the text. The concentration of  $Hg(C_6H_6)_2(GaCl_4)_2$  at any time ( $t$ ) may be determined from the relative rate of H/D exchange, assuming it is a combination of two independent reactions (eqs 6 and 9). If the concentration of  $Hg(C_6H_6)_2(GaCl_4)_2$  as a function of time is known, then a standard first-order plot may be drawn and the  $k_{ex}$  obtained (Figure 7). Measurement of the temperature dependence for  $k_{ex}$  allows for the determination of  $\Delta H^\ddagger$  and  $\Delta S^\ddagger$  in the normal manner. Errors were calculated by standard methods.

**$Hg(C_{10}H_8)_2(GaCl_4)_2$ .**  $Hg(C_6H_5Me)_2(GaCl_4)_2$  (0.50 g, 0.062 mmol) was dissolved in toluene (20 mL), and the solution was heated slightly to ensure complete dissolution. A large excess of naphthalene (7.93 g, 0.062 mol) was added to the warm yellow solution, resulting in a red solution. The reaction flask was covered in aluminum foil to prevent decomposition of the light-sensitive mercury complexes and was allowed to cool to room temperature. The solution was stirred for 12 h to ensure that the ligand exchange between  $C_6H_5Me$  and naphthalene went to completion. Upon cooling to  $-24$   $^{\circ}C$ , orange precipitate formed. Yield: 80%. MS (EI, %):  $m/z$  ( $M^+$ , 100).  $^{13}C$  CPMS NMR (50.32 MHz):  $\delta$  145 (1C, 1-C), 140 (1C, 10-C), 136 (3C, 4-C, 6-C, 9-C), 134 (1C, 5-C), 130 (2C, 7-C, 8-C), 127 (1C, 3-C), 119 (1C,  $Hg\cdots CH$ ).

**Computational Methods.** All density functional calculations were carried out using a Gaussian-98 suite.<sup>19</sup> Complete geometry optimizations were performed at the B3LYP20 level using the 6-31G\*\* basis set for C and H only and the Stuttgart RLC ECP basis set for Hg, Cl, and Ga.  $C_2$  symmetry was imposed. Vibrational frequencies were then evaluated for naphthalene complexes to verify the existence of the true potential minimum and to determine zero-point energies.  $^{13}C$  NMR chemical shifts for  $Hg(C_{10}H_8)_2(GaCl_4)_2$  were calculated at the same level of theory.

**Acknowledgment.** Financial support for this work is provided by the Robert A. Welch Foundation and the Petroleum Research Fund. The Bruker Avance 200 and 500 NMR spectrometers were purchased with funds from ONR Grant N00014-96-1-1146 and NSF Grant CHE-9708978, respectively.

**Supporting Information Available:** Structural parameters and energies for optimized structures from DFT calculations. Ordering information is given on any current masthead page. This material is available free of charge via the Internet at <http://pubs.acs.org>.

JA0206590

- (19) Frisch, M. J.; Trucks, G. W.; Schlegel, H. B.; Scuseria, G. E.; Robb, M. A.; Cheeseman, J. R.; Zakrzewski, V. G.; Montgomery, J. A., Jr.; Stratmann, R. E.; Burant, J. C.; Dapprich, S.; Millam, J. M.; Daniels, A. D.; Kudin, K. N.; Strain, M. C.; Farkas, O.; Tomasi, J.; Barone, V.; Cossi, M.; Cammi, R.; Mennucci, B.; Pomelli, C.; Adamo, C.; Clifford, S.; Ochterski, J.; Petersson, G. A.; Ayala, P. Y.; Cui, Q.; Morokuma, K.; Malick, D. K.; Rabuck, A. D.; Raghavachari, K.; Foresman, J. B.; Cioslowski, J.; Ortiz, J. V.; Baboul, A. G.; Stefanov, B. B.; Liu, G.; Liashenko, A.; Piskorz, P.; Komaromi, I.; Gomperts, R.; Martin, R. L.; Fox, D. J.; Keith, T.; Al-Laham, M. A.; Peng, C. Y.; Nanayakkara, A.; Challacombe, M.; Gill, P. M. W.; Johnson, B.; Chen, W.; Wong, M. W.; Andres, J. L.; Gonzalez, C.; Head-Gordon, M.; Replogle, E. S.; Pople, J. A. *Gaussian-98*, revision A.9; Gaussian, Inc.: Pittsburgh, PA, 1998.
- (20) (a) Becke, A. D. *J. Chem. Phys.* **1993**, *98*, 5648. (b) Stephens, P. J.; Devlin, C. F.; Chabalowski, C. F.; Frisch, M. J. *J. Phys. Chem.* **1994**, *98*, 11623. (c) Lee, C.; Yang, W.; Parr, R. G. *Phys. Rev.* **1988**, *B37*, 785.